

Article

Features of Fabrication of Titanium Dioxide Based Coatings for Non-Lithographic Template Electrochemical Synthesis of Micron Metal Particle Arrays

Andrey Yu Arbenin ^{1,*}, Elena G. Zemtsova ¹, Evgeniy V. Orekhov ¹, Daria N. Sokolova ¹, Polina I. Baburova ¹, Alexey A. Petrov ¹, Vladimir E. Gaishun ² and Vladimir M. Smirnov ¹

¹ St. Petersburg State University, 7/9 Universitetskaya nab., 199034 Saint Petersburg, Russia; ezimtsova@yandex.ru (E.G.Z.); zeka@list.ru (E.V.O.); darya.sokolova.2014@mail.ru (D.N.S.); polly113@mail.ru (P.I.B.); st068921@student.spbu.ru (A.A.P.); vms11@yandex.ru (V.M.S.)

² Francisk Skarina Gomel State University, 104 Sovetskaya Str., 246019 Gomel, Belarus; vgaishun@gsu.by

* Correspondence: aua47@yandex.ru

Abstract: This work is devoted to the development of non-lithographic template methods of synthesis. These methods have a significant advantage in terms of structure formation: there is no need to design and produce masks, which greatly simplifies the process, and more of them can work with nonplanar substrates. The purpose of this study was to reveal the conditions for the synthesis of titanium dioxide xerogel films of different topologies as well as to develop a technique for non-lithographic template electrochemical synthesis of micron metal particles arrays and to study the structure of the resulting coatings. The films were deposited on the surface of substrates via dip coating. Specific topology of the films was achieved by template sol-gel synthesis. Their structures were analyzed by SEM and XRD. Template synthesis of metal micro particles were realized by pulsed electrochemical deposition of metals into the perforations of xerogel films. Obtained materials were analyzed by SEM and XRD; the element distribution on the surface was determined by the EDS detector of SEM. Based on the analysis results, we suggest the mechanisms of formation of the xerogel topology and proved the efficiency of pulsed electrodeposition for template synthesis of micron particles arrays.

Keywords: template synthesis; sol-gel; xerogel; thin films; pores; dip coating; electrochemical deposition; metal particles



Citation: Arbenin, A.Y.; Zemtsova, E.G.; Orekhov, E.V.; Sokolova, D.N.; Baburova, P.I.; Petrov, A.A.; Gaishun, V.E.; Smirnov, V.M. Features of Fabrication of Titanium Dioxide Based Coatings for Non-Lithographic Template Electrochemical Synthesis of Micron Metal Particle Arrays. *Gels* **2021**, *7*, 202. <https://doi.org/10.3390/gels7040202>

Academic Editor:
Annarosa Gugliuzza

Received: 8 October 2021
Accepted: 4 November 2021
Published: 7 November 2021

Publisher's Note: MDPI stays neutral with regard to jurisdictional claims in published maps and institutional affiliations.



Copyright: © 2021 by the authors. Licensee MDPI, Basel, Switzerland. This article is an open access article distributed under the terms and conditions of the Creative Commons Attribution (CC BY) license (<https://creativecommons.org/licenses/by/4.0/>).

1. Introduction

An important direction in materials science is surface engineering, which is aimed at the formation of materials with a given topology and functional properties. There are two approaches to produce required topology: methods of forced organization and self-organization methods. Both methods have been developed in recent decades. A more common method of forced synthesis is lithography [1–3]. This method is widespread because it is very convenient for the production of electronic components necessary for the production of computers and other electronic devices without which we cannot imagine our lives. Photolithography [4] is most commonly used in the microelectronics industry. The topology obtained with this technology is formed due to a photomask [5], a replica of which is created on the surface of a substrate by illuminating the photoresist [6] deposited on the surface through this photomask. After the photoresist has been developed, it is possible to etch the substrate or apply layers to obtain the desired topology.

Self-organization methods have a significant advantage in terms of structure formation: there is no need to design and produce masks, which greatly simplifies the process. In the field of chemical materials science, many objects are obtained by self-organization, for example, micelles [7], liquid crystals [8], self-organizing monolayers [9], anodic mesoporous films [10], metal-organic frameworks [11], polymer microphase separations [12],

Blodgett–Langmuir films [13], and colloidal crystals [14]. Many self-organizing objects can act as templates to produce materials with a given structure, for example, micelles are used for producing nanoparticles [15–17], micelles assembled in liquid crystal are used for producing mesoporous materials [18–20], and anodized or liquid crystal templated mesoporous materials are often used as a template for producing nanoparticles [21–23], nanowires [24–26], etc.

Many methods based on self-organization are suitable for creating not only bulk or dispersed materials, but also coatings with a given topology, making them competitive with lithography. For example, a macroporous ordered polymer coating can be obtained by template synthesis using a spin-coated colloidal crystal [27], and an array of silver nanorods oriented normally to the substrate can be obtained by template electrochemical synthesis using anodic films [28]. There are many such coatings and many of them are useful for practical applications in various fields, for example, in optics [29–31], microelectromechanical systems [32–34], sensors [35–37], and medicine [38–40].

This paper presents the results of a study of the possibility of synthesizing perforated films of titanium oxide xerogel on the surface of an electrically conductive substrate with a topology arising due to the microphase separation of polyethylene glycol introduced into the initial sol. The obtained films were used to develop a technique for template electrochemical synthesis of metal microparticle arrays.

2. Materials and Methods

In this study, monocrystalline silicon wafers KEF (4" × 525 μm) with an orientation (111) produced by Ostek-INTEGRA LLC, Moscow, Russia was used as a substrate. To prepare samples for xerogel application, the original silicon wafers were scribed with a diamond tool and bent to split into separate rectangular wafers of a size approximately 10 mm × 50 mm.

An alcoholic solution of titanium isopropoxide with various additives was used as a synthetic solution for the template coating: isopropanol puriss (Vecton LLC, Moscow, Russia), titanium isopropoxide 99% (Sigma Aldrich), diethanolamine 99% (Sigma Aldrich), polyethylene glycol 99% Mw 20,000 (Dalton Merk). The films were coated on a KSV NIMA single vessel dip coater. For further electrochemical synthesis, a 6 mm × 12 mm working window was created, and the rest of the surface was covered with an LF32 electrical insulating chemical-resistant varnish by Plastpolymer-Prom LLC. This avoids metal deposition on the unpolished side of the wafers and on the sharp edges of the chips.

For the template electrochemical deposition of arrays of metal microparticles, silver, nickel, and copper water-based electrolytes were used, which included: silver nitrate AR (Vecton LLC, Moscow, Russia), copper sulfate pentahydrate puriss (Vecton LLC, Moscow, Russia), nickel sulfate hexahydrate puriss (Vecton LLC, Moscow, Russia), nickel chloride hexahydrate puriss (Vecton LLC, Moscow, Russia), boric acid puriss (Vecton LLC, Moscow, Russia), sulfosalicylic acid puriss (Vecton LLC, Moscow, Russia), and aqueous ammonia 25% mass. pure (Vecton LLC, Moscow, Russia). An electrochemical cell with a counter electrode corresponding to the electrolyte (Ag, Ni, Cu) and a magnetic stirrer was used for deposition. A silver chloride electrode ESr-10102 Izmtech LLC, Moscow, Russia was used to create a reference potential. To generate electrical pulses required for the electrochemical deposition of metals, a potentiostat-galvanostat Elins P-45X FRA-24 M was used.

The structures and element distributions in the coatings were studied using a Zeiss Merlin scanning electron microscope with an Oxford Instruments INCAx-act energy dispersive spectrometer. The phase analysis of the obtained coatings was performed using an X-ray diffractometer (Rigaku MiniFlex II) with CuK α radiation.

3. Results and Discussion

The first stage of the work involved the deposition of a titanium dioxide xerogel film on a silicon substrate. The synthetic solution was a mixture of titanium isopropoxide, isopropanol, diethanolamine, and water in the following mass ratios TTIP/i-

PrOH/DEA/H₂O = 227/773/105/36. The coating was applied using a dip coater at a withdrawal speed of 100 mm/min at ambient temperature. The substrate was then placed on a hot plate at 100 °C, washed with boiling water, and dried by repeated heating on a hot plate. Thus, sample #1 was obtained, which as shown by SEM, had a uniform film (Figure 1A) consisting of the xerogel, as evidenced by the globular nanometer structure of the film (Figure 1B). The results correlated well with the literature data [41].

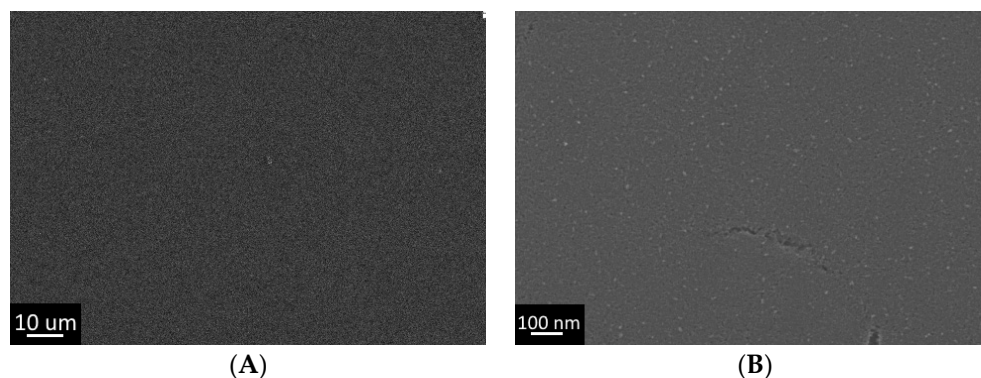


Figure 1. Structure of the coating obtained from an alcoholic solution of titanium isopropoxide by dip coating (Sample #1):(A) Low resolution SEM; (B) High resolution SEM.)

The next step was to investigate the formation of the xerogel film micron structure by introducing polyethylene glycol into the synthetic solution. When PEG 20,000 at a concentration of 2.5 wt.%, was introduced into the synthetic solution, there was no complete dissolution. After heating to 80 °C, the solution became completely transparent. During film deposition by dip coating (withdrawal speed was 100 mm/min as in the case of the first sample), the reverse process of polymer separation into a separate phase occurred, which resulted in a film with a micron relief after gel conversion into xerogel (Figure 2).

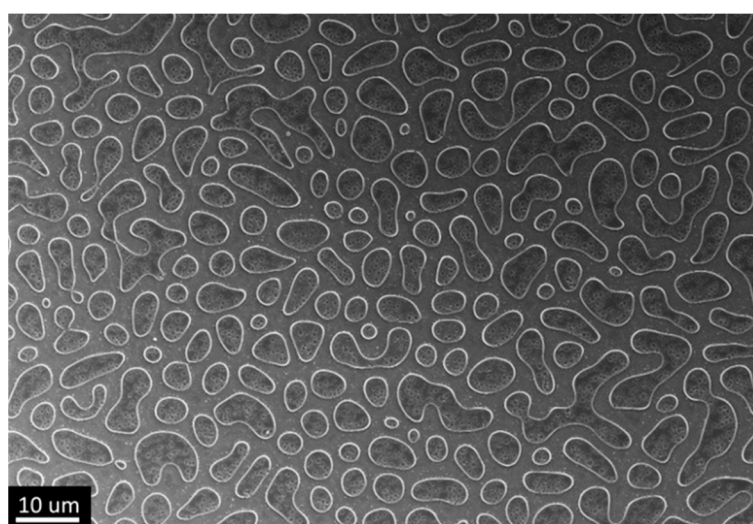


Figure 2. Structure of the coating obtained from an alcoholic solution of titanium isopropoxide at a temperature of 80 °C by dip coating with PEG 20,000 (Sample #2).

In the application of sol-gel coatings, polyethylene glycol as well as a number of other polymer additives is used as a plasticizer that protects films from cracking [42]. However, in some cases during sol-gel synthesis in the presence of polymers, a process of microphase separation can occur [43–45]. This process can fundamentally change product properties by precipitating the polymer phase, for example, causing macropores or oblong cracks in

xerogel films [46,47]. In this case, the process of the formation of the separated polymer structure is dynamic, and at speeds commensurate with the formation of the gel, there is a possibility to adjust the geometry of the product from individual inclusions to a continuous mesh. Additionally, during aggregation, the structure inversion is possible, when there is a complete separation of parts of the previously continuous gel into separate areas; this process is called spheroidization by the authors [48]. The obtained structure is very similar to the spheroidization process, but the term is not applicable to this object due to the fact that the process took place in a thin film rather than in a volume, and the size of the structures was much larger than the film thickness. However, the formation of separated titanium oxide gel regions can be explained by the proposed mechanism.

Decreasing the temperature of the reaction solution led to the inversion of the film: at 65 °C, deposition under the same synthetic conditions led to the formation of a titanium oxide xerogel film with wells, which apparently were formed due to PEG precipitation (Figure 3).

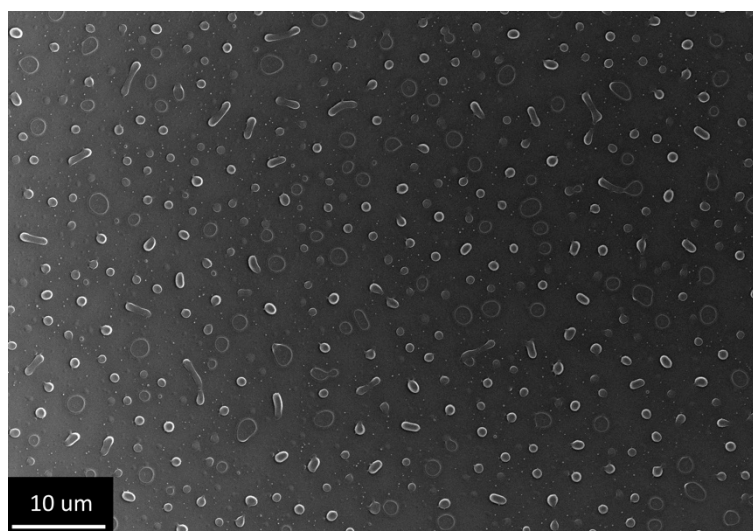


Figure 3. Structure of the film obtained by dip coating from an alcoholic solution of titanium isopropoxide using PEG 20,000 at 65 °C (Sample #3).

At the same time, peeling meniscuses of xerogel could be observed in the pores. These structures were not complete perforations, but rather wells; similar objects can be found in the literature [49]. Due to the presence of an insulator at the bottom of the well, they are not interesting for electrochemical template synthesis. For removing meniscuses, it was decided to use shock drying of freshly deposited gels. Rapid drying of gels can lead to cracking [40,50,51]. Additionally, due to the presence of extended objects, it was decided to speed up the process of PEG separation as much as possible in order to avoid its aggregation into oblong agglomerations or a single grid. For this purpose, we came very close to the cloud point: the film application process was carried out from a 45 °C solution followed by shock drying in hot plate mode at 400 °C. This approach made it possible to obtain a titanium oxide xerogel film with circular perforations without aggregation and the presence of meniscuses in the pores. However, during the shock drying process, the edges of the perforations were cracked (Figure 4), thus forming star-shaped perforations.

X-ray diffraction study of the sample showed weak rutile (TiO_2) phase peaks against the background of the intense Si (111) substrate peak (Figure 5).

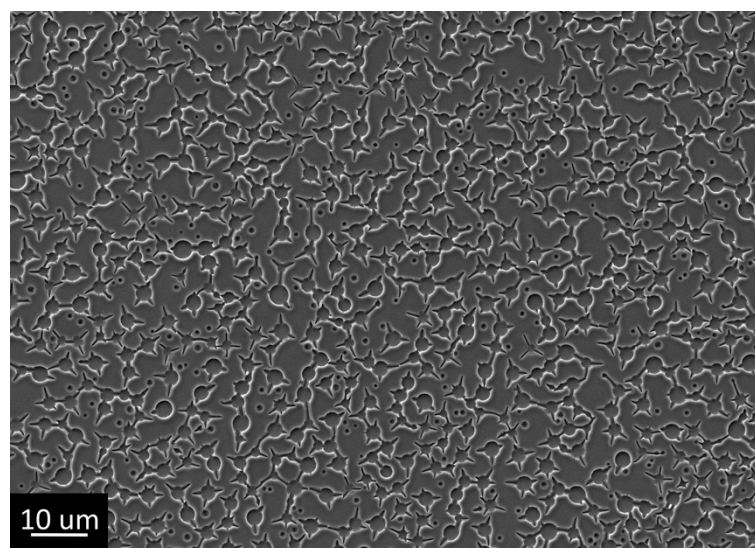


Figure 4. Structure of the film obtained by dip coating from an alcoholic titanium isopropoxide solution using PEG 20,000 at 45 °C with post-synthetic hot plate treatment at 400 °C (Sample #4).

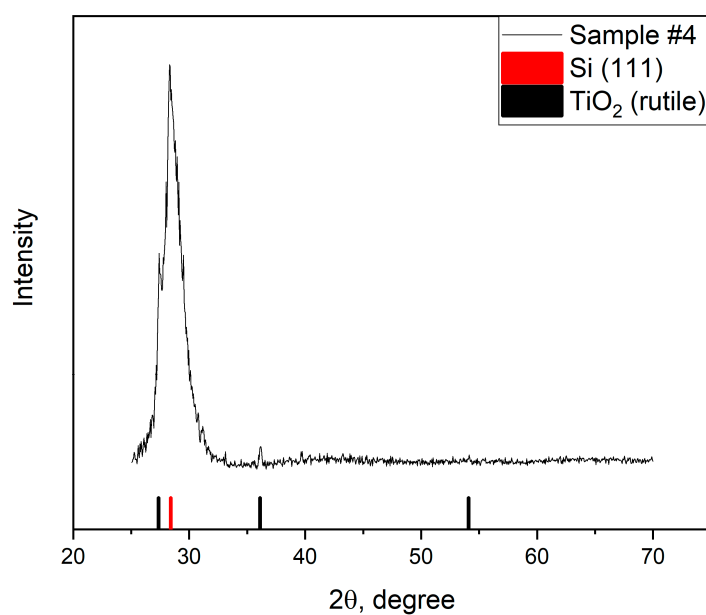


Figure 5. X-ray diffractogram of sample #4.

Table 1 summarizes the synthesis conditions and structures of the obtained coatings.

Table 1. Synthetic conditions and structures of the xerogel coatings.

Sample	ω PEG 2000, %	t of Solution, °C	Shock Drying	Structure
1	0	ambient	–	Uniform film
2	2.5	80	–	Island-like coating
3	2.5	65	–	Film with wells
4	2.5	45	+	Film with perforations

The developed technique for producing perforated films is interesting for template lithography-free electrochemical synthesis of arrays of micron-sized metal particles because the film with low conductivity has through-micron perforations that reveal areas of the electrically conductive substrate, which is similar to lithographic masks for metallization [52].

To investigate the possibility of using the developed film as a template for the electrochemical synthesis of micron metal particles, electrochemical deposition of silver in the pulse mode was carried out: pauses between pulses allowed us to restore the concentration of silver ions in the deposition zones; and the reverse pulse allowed us to remove the charge of the double electric layer. This approach can be found in the literature for the template synthesis of metal nanowires in the pores of anodized aluminum [25,53]. As a result of 1250 deposition cycles (Table 2), a silver deposit structure was obtained, which rather precisely reproduced the micron texture of the xerogel film (Figure 6).

Table 2. Sequence of the applied potentials used for template silver electrochemical deposition.

E, V	−1	0.3	2	0
τ , ms	5	3	10	65

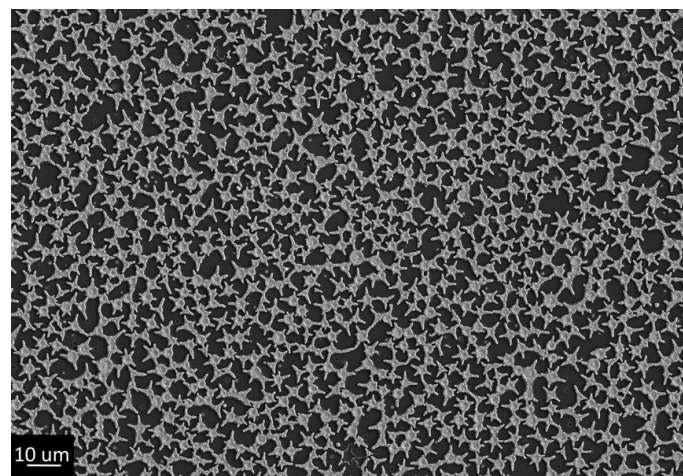


Figure 6. Scanning electron microscopy of silver microparticle array obtained with template electrochemical synthesis.

The presence of silver in these microparticles was proven by X-ray diffraction (Figure 7).

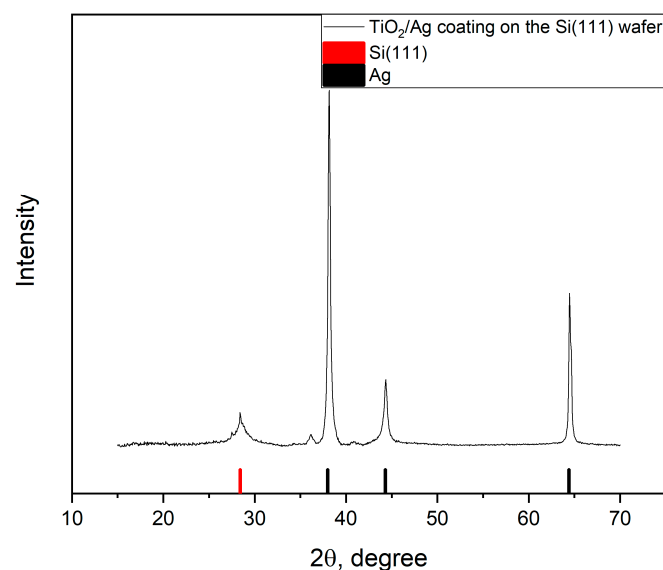


Figure 7. X-ray diffraction of the sample with the silver microparticle array obtained with template electrochemical synthesis.

The efficiency of the developed template synthesis was proven by the elemental mapping detected by SEM EDS (Figure 8).

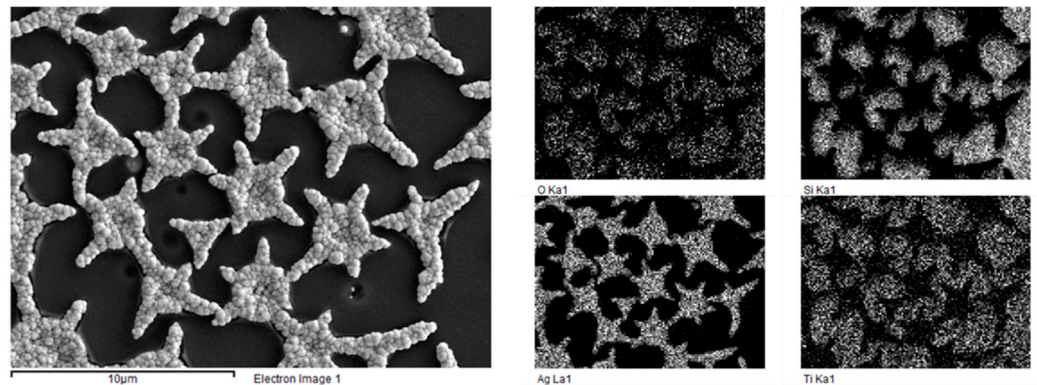


Figure 8. Element distribution on the surface of the sample with the silver microparticle array obtained with template electrochemical synthesis.

Microscopy of the sample chip revealed that the resulting coating had a thickness of several hundred nanometers, with silver particles elevated above the xerogel film (Figure 9). This object had a two-level hierarchy of relief, which is interesting from the point of view of materials science, for example, for the creation of materials for bone implantation, where such topology is very promising for the improvement in biomedical properties [54].

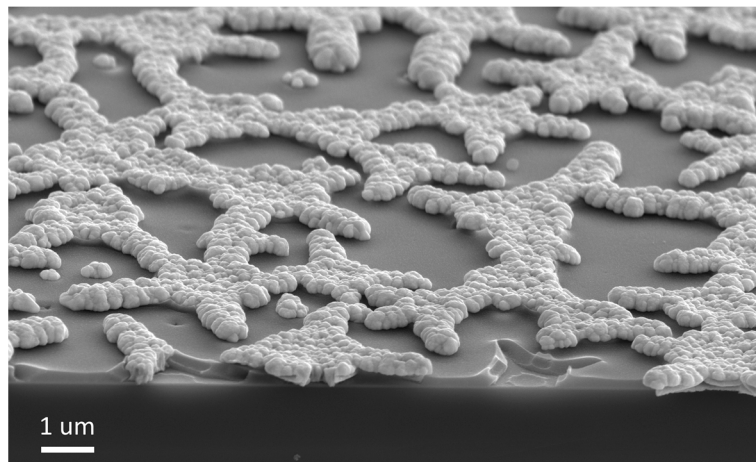


Figure 9. Scanning electron microscopy of the chip of the sample with a silver microparticle array obtained with template electrochemical synthesis.

Furthermore, the possibility of applying the developed approach to create arrays of micron particles of other metals was investigated. Nickel and copper were chosen for the development of the technique, since these metals are often used to create electrochemical sensors [55,56]. As a result of a series of experiments, electrolytes and regimes suitable for template electrochemical deposition of these metals were found.

Nickel deposition from an aqueous electrolyte of the composition—nickel sulfate 1.5% wt, boric acid 3% wt, in the pulse mode (6 V-10 ms, 130 ms relaxation)—produced an array of nickel microparticles that replicated the shape of perforations of the xerogel film. X-ray phase analysis confirmed the presence of the nickel phase; however, in addition to the metallic nickel, a nickel (II) oxide phase was detected, which may be due to oxidation of the deposited nickel in contact with the atmosphere (Figure 10).

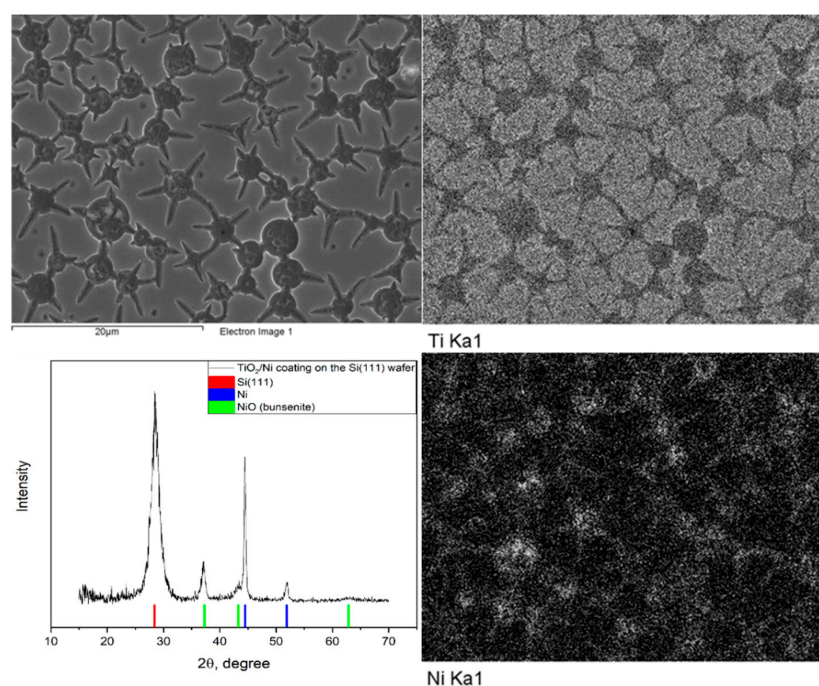


Figure 10. Results of the SEM EDS XRD analysis of samples with the arrays of nickel microparticles obtained by template electrochemical synthesis.

Similar results were obtained during copper deposition from an aqueous electrolyte consisting of copper sulfate 5% wt, and boric acid 1% wt in the pulse mode (-0.3 V-3 ms, 3 V-10 ms and 200 ms relaxation). As in the case of electrochemical nickel deposition, X-ray phase analysis revealed oxidation products of copper, apparently formed in contact with the atmosphere (Figure 11).

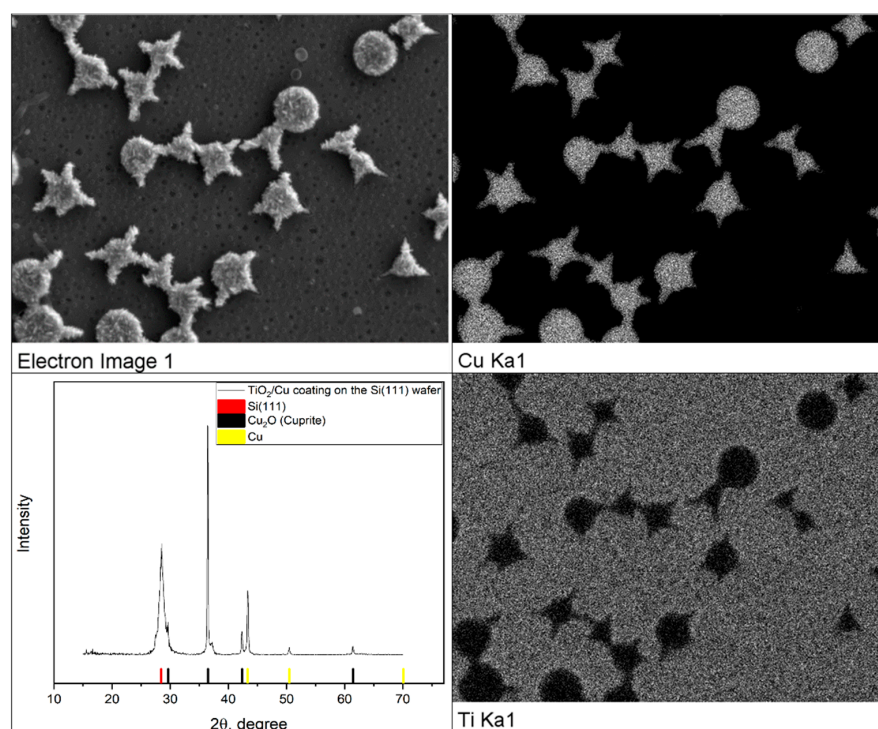


Figure 11. Results of SEM EDS XRD analysis of samples with the arrays of copper microparticles obtained by template electrochemical synthesis.

The developed method refers to non-lithographic methods, which simplifies the technology of obtaining the required topology of the substrate surface. The combination of sol-gel template dip coating and template electrochemical deposition allows for the production of arrays of micron particles of various metals on the surface of a conductive substrate.

4. Conclusions

As a result of the study, the possibility of synthesizing thin films of mesoporous TiO₂ xerogel by the sol-gel method using dip coating technology with micron star-shaped perforations resulting from the use of a template-PEG-20000—was experimentally shown.

Due to perforations, these films can be used for the electrochemical template synthesis of arrays of micron-sized metallic particles (Ag, Ni, Cu) immobilized on the surface of substrates. It has been experimentally proven that the replication of the texture of the electrochemical deposit template occurs only when using the pulsed deposition mode.

Author Contributions: A.Y.A., main idea development, template synthesis.; E.G.Z., reagent preparation; E.V.O., preparation of perforated films; D.N.S., dip coating of star-like perforated films; P.I.B., electrochemical deposition; A.A.P., consult in electrochemical area; V.E.G., consult in sol-gel area; V.M.S., literature analysis. All authors have read and agreed to the published version of the manuscript.

Funding: The study was supported by St. Petersburg State University (ID: 74883303).

Data Availability Statement: Not applicable.

Acknowledgments: The research was carried out using the equipment of the resource centers of the St. Petersburg State University Scientific Park “X-ray diffraction research methods” and “Nanotechnology”.

Conflicts of Interest: The authors declares no conflict of interest.

References

1. Kim, P.; Kwon, K.W.; Park, M.C.; Lee, S.H.; Kim, S.M.; Suh, K.Y. Soft lithography for microfluidics: A review. *Biochip J.* **2008**, *2*, 1–11.
2. Schiff, H. Nanoimprint lithography: An old story in modern times? A review. *J. Vac. Sci. Technol. B* **2008**, *26*, 458–480. [[CrossRef](#)]
3. Watt, F.; Bettiol, A.; van Kan, J.A.; Teo, E.J.; Breese, M.B.H. Ion beam lithography and nanofabrication: A review. *Int. J. Nanosci.* **2005**, *4*, 269–286. [[CrossRef](#)]
4. Seisyan, R.P. Nanolithography in microelectronics: A review. *Tech. Phys.* **2011**, *56*, 1061–1073. [[CrossRef](#)]
5. Gallagher, E.; Hibbs, M. Masks for micro- and nanolithography. In *Nanolithography*; Woodhead Publishing: Cambridge, UK, 2014; pp. 158–178. [[CrossRef](#)]
6. Lin, Q. Properties of Photoresist Polymers. In *Physical Properties of Polymers Handbook*; Springer: New York, NY, USA, 2007; pp. 965–979.
7. Menger, F.M. The structure of micelles. *Acc. Chem. Res.* **1979**, *12*, 111–117. [[CrossRef](#)]
8. Priestly, E. *Introduction to Liquid Crystals*; Springer Science & Business Media: Cham, Switzerland, 2012.
9. Rohwerder, M.; de Weldige, K.; Vago, E.; Viehhaus, H.; Stratmann, M. Adsorption of self-assembled monolayers of mercaptan on gold. *Thin Solid Films* **1995**, *264*, 240–245. [[CrossRef](#)]
10. Michalska-Domańska, M.; Norek, M.; Stepniowski, W.; Budner, B. Fabrication of high quality anodic aluminum oxide (AAO) on low purity aluminum—A comparative study with the AAO produced on high purity aluminum. *Electrochim. Acta* **2013**, *105*, 424–432. [[CrossRef](#)]
11. Shekhah, O.; Liu, J.; Fischer, R.A.; Wöll, C. MOF thin films: Existing and future applications. *Chem. Soc. Rev.* **2011**, *40*, 1081–1106. [[CrossRef](#)]
12. Spontak, R.J.; Williams, M.C.; Agard, D.A. Three-dimensional study of cylindrical morphology in a styrene-butadiene-styrene block copolymer. *Polymer* **1988**, *29*, 387–395. [[CrossRef](#)]
13. Roberts, G. (Ed.) *Langmuir-Blodgett Films*; Springer Science & Business Media: New York, NY, USA, 2013.
14. Kumacheva, E.; Garstecki, P.; Wu, H.; Whitesides, G.M. Two-Dimensional Colloid Crystals Obtained by Coupling of Flow and Confinement. *Phys. Rev. Lett.* **2003**, *91*, 128301. [[CrossRef](#)]
15. Li, Y.; Zaluzhna, O.; Tong, Y.J. Critical Role of Water and the Structure of Inverse Micelles in the Brust-Schiffrin Synthesis of Metal Nanoparticles. *Langmuir* **2011**, *27*, 7366–7370. [[CrossRef](#)] [[PubMed](#)]
16. Uskokovi, V.; Drogenik, M. Synthesis of materials within reverse micelles. *Surf. Rev. Lett.* **2005**, *12*, 239–277. [[CrossRef](#)]
17. Smetana, A.B.; Wang, J.S.; Boeckl, J.; Brown, G.J.; Wai, C.M. Fine-Tuning Size of Gold Nanoparticles by Cooling during Reverse Micelle Synthesis. *Langmuir* **2007**, *23*, 10429–10432. [[CrossRef](#)] [[PubMed](#)]

18. Kresge, C.T.; Leonowicz, M.E.; Roth, W.; Vartuli, J.C.; Beck, J.S. Ordered mesoporous molecular sieves synthesized by a liquid-crystal template mechanism. *Nature* **1992**, *359*, 710–712. [[CrossRef](#)]
19. Kruk, M.; Jaroniec, M.; Ko, C.H.; Ryoo, R. Characterization of the Porous Structure of SBA-15. *Chem. Mater.* **2000**, *12*, 1961–1968. [[CrossRef](#)]
20. Alfredsson, V.; Anderson, M.W. Structure of MCM-48 Revealed by Transmission Electron Microscopy. *Chem. Mater.* **1996**, *8*, 1141–1146. [[CrossRef](#)]
21. Zemtsova, E.G.; Arbenin, A.Y.; Ponomareva, A.N.; Smirnov, V.M. Synthesis of Magnetite Nanoparticles in Pores of Mesoporous Silica MSM-41 and Study of Their Magnetic Properties. *Russ. J. Gen. Chem.* **2018**, *88*, 2216–2218. [[CrossRef](#)]
22. Zemtsova, E.G.; Arbenin, A.Y.; Galiullina, L.F.; Ponomareva, A.N.; Sokolova, D.N.; Smirnov, V.M. Regulation of the size of metal iron nanoparticles in channels of mesoporous silica matrices (MCM-41, SBA-15) and structure and magnetic properties of the received nanocomposites MCM-41/FeO and SBA-15/FeO. *J. Nanoparticle Res.* **2020**, *22*, 255. [[CrossRef](#)]
23. Okumura, M.; Tsubota, S.; Iwamoto, M.; Haruta, M. Chemical Vapor Deposition of Gold Nanoparticles on MCM-41 and Their Catalytic Activities for the Low-temperature Oxidation of CO and of H₂. *Chem. Lett.* **1998**, *27*, 315–316. [[CrossRef](#)]
24. Liu, Z.; Sakamoto, Y.; Ohsuna, T.; Hiraga, K.; Terasaki, O.; Ko, C.H.; Shin, H.J.; Ryoo, R. TEM Studies of Platinum Nanowires Fabricated in Mesoporous Silica MCM-41. *Angew. Chem.* **2000**, *39*, 3107–3110. [[CrossRef](#)]
25. Kim, K.; Kim, M.; Cho, S.M. Pulsed electrodeposition of palladium nanowire arrays using AAO template. *Mater. Chem. Phys.* **2006**, *96*, 278–282. [[CrossRef](#)]
26. de la Prida, V.; Hernández-Vélez, M.; Cervera, M.; Pirotta, K.; Sanz, R.; Navas, D.; Asenjo, A.; Aranda, P.; Ruiz-Hitzky, E.; Batallán, F.; et al. Magnetic behaviour of arrays of Ni nanowires by electrodeposition into self-aligned titania nanotubes. *J. Magn. Magn. Mater.* **2005**, *294*, e69–e72. [[CrossRef](#)]
27. Jiang, P.; McFarland, M.J. Large-Scale Fabrication of Wafer-Size Colloidal Crystals, Macroporous Polymers and Nanocomposites by Spin-Coating. *J. Am. Chem. Soc.* **2004**, *126*, 13778–13786. [[CrossRef](#)]
28. Sun, X.-Y.; Xu, F.-Q.; Li, Z.-M.; Zhang, W.-H. Cyclic voltammetry for the fabrication of high dense silver nanowire arrays with the assistance of AAO template. *Mater. Chem. Phys.* **2005**, *90*, 69–72. [[CrossRef](#)]
29. Qin, Y.; Kong, X.-T.; Wang, Z.; Govorov, A.O.; Kortshagen, U.R. Near-Infrared Plasmonic Copper Nanocups Fabricated by Template-Assisted Magnetron Sputtering. *ACS Photon.* **2017**, *4*, 2881–2890. [[CrossRef](#)]
30. Foss, C.A.; Tierney, M.J.; Martin, C.R. Template synthesis of infrared-transparent metal microcylinders: Comparison of optical properties with the predictions of effective medium theory. *J. Phys. Chem.* **1992**, *96*, 9001–9007. [[CrossRef](#)]
31. Takeoka, Y.; Watanabe, M. Template Synthesis and Optical Properties of Chameleonic Poly(N-isopropylacrylamide) Gels Using Closest-Packed Self-Assembled Colloidal Silica Crystals. *Adv. Mater.* **2003**, *15*, 199–201. [[CrossRef](#)]
32. Wasim, M.F.; Ashraf, M.W.; Tayyaba, S.; Nazir, A.S. Simulation and synthesis of ZnO nanorods on AAO nano porous template for use in a mems devices. *Dig. J. Nanomater. Biostruct.* **2019**, *14*, 559–567.
33. Ali, B.; Ashraf, M.W.; Tayyaba, S. Simulation, Fuzzy Analysis and Development of ZnO Nanostructure-based Piezoelectric MEMS Energy Harvester. *Energies* **2019**, *12*, 807. [[CrossRef](#)]
34. Lv, H.; Liu, S. Preparation and Analysis of Porous Anodic Alumina Template on Silicon Substrate. *Mater. Manuf. Process.* **2015**, *31*, 157–161. [[CrossRef](#)]
35. Caihong, W.; Chu, X.; Wu, M. Highly sensitive gas sensors based on hollow SnO₂ spheres prepared by carbon sphere template method. *Sens. Actuators B Chem.* **2007**, *120*, 508–513. [[CrossRef](#)]
36. Arbenin, A.; Zemtsova, E.G.; Ermakov, S.S.; Gas'Kov, A.M.; I Baburova, P.; Sokolova, D.N.; Yaroshenko, S.V.; Smirnov, V.M. Three-component working electrode micron-sized Ag particles/tiO₂ layer/Ti: Template electrochemical synthesis and potential use as electrochemical sensor for glutathione detection. *Mater. Res. Express* **2020**, *7*, 035401. [[CrossRef](#)]
37. Ding, D.; Chen, Z.; Rajaputra, S.; Singh, V. Hydrogen sensors based on aligned carbon nanotubes in an anodic aluminum oxide template with palladium as a top electrode. *Sens. Actuators B Chem.* **2007**, *124*, 12–17. [[CrossRef](#)]
38. Ma, J.; Wang, J.; Ai, X.; Zhang, S. Biomimetic self-assembly of apatite hybrid materials: From a single molecular template to bi-/multi-molecular templates. *Biotechnol. Adv.* **2014**, *32*, 744–760. [[CrossRef](#)]
39. Wu, K.; Tao, J.; Liao, Q.; Chen, S.; Wan, W. Intracellular microtubules as nano-scaffolding template self-assembles with conductive carbon nanotubes for biomedical device. *Mater. Sci. Eng. C* **2020**, *113*, 110971. [[CrossRef](#)]
40. Zemtsova, E.G.; Arbenin, A.Y.; Yudincheva, N.M.; Valiev, R.Z.; Orekhov, E.V.; Smirnov, V.M. Bioactive Coating with Two-Layer Hierarchy of Relief Obtained by Sol-Gel Method with Shock Drying and Osteoblast Response of Its Structure. *Nanomaterials* **2017**, *7*, 323. [[CrossRef](#)]
41. Takahashi, Y.; Matsuoka, Y. Dip-coating of TiO₂ films using a sol derived from Ti(O-i-Pr)₄-diethanolamine-H₂O-i-PrOH system. *J. Mater. Sci.* **1988**, *23*, 2259–2266. [[CrossRef](#)]
42. Catauro, M.; Papale, F.; Piccirillo, G.; Bollino, F. PEG-based organic-inorganic hybrid coatings prepared by the sol-gel dip-coating process for biomedical applications. *Polym. Eng. Sci.* **2017**, *57*, 478–484. [[CrossRef](#)]
43. Lu, X.; Hasegawa, G.; Kanamori, K.; Nakanishi, K. Hierarchically porous monoliths prepared via sol-gel process accompanied by spinodal decomposition. *J. Sol.-Gel Sci. Technol.* **2020**, *95*, 530–550. [[CrossRef](#)]
44. Lei, B.; Chen, X.; Han, X.; Zhou, J. Versatile fabrication of nanoscale sol-gel bioactive glass particles for efficient bone tissue regeneration. *J. Mater. Chem.* **2012**, *22*, 16906–16913. [[CrossRef](#)]

45. Chiang, C.-L.; Ma, C.-C.M.; Wu, D.-L.; Kuan, H.-C. Preparation, characterization, and properties of novolac-type phenolic/SiO₂ hybrid organic-inorganic nanocomposite materials by sol-gel method. *J. Polym. Sci. Part A Polym. Chem.* **2003**, *41*, 905–913. [[CrossRef](#)]
46. Sonawane, R.S.; Kale, B.B.; Dongare, M.K. Preparation and photo-catalytic activity of Fe-TiO₂ thin films prepared by sol-gel dip coating. *Mater. Chem. Phys.* **2004**, *85*, 52–57. [[CrossRef](#)]
47. Kajihara, K.; Nakanishi, K. Macroporous morphology of titania films prepared by sol-gel dip-coating method from a system containing poly(ethylene glycol) and poly(vinylpyrrolidone). *J. Mater. Res.* **2001**, *16*, 58–66. [[CrossRef](#)]
48. Nakanishi, K.; Tanaka, N. Sol-Gel with Phase Separation. Hierarchically Porous Materials Optimized for High-Performance Liquid Chromatography Separations. *Acc. Chem. Res.* **2007**, *40*, 863–873. [[CrossRef](#)] [[PubMed](#)]
49. Calderon-Moreno, J.; Preda, S.; Predoana, L.; Zaharescu, M.; Anastasescu, M.; Nicolescu, M.; Stoica, M.; Stroescu, H.; Gartner, M.; Buiu, O.; et al. Effect of polyethylene glycol on porous transparent TiO₂ films prepared by sol-gel method. *Ceram. Int.* **2014**, *40*, 2209–2220. [[CrossRef](#)]
50. Barati, N.; Sani, M.F.; Ghasemi, H.; Sadeghian, Z.; Mirhoseini, S. Preparation of uniform TiO₂ nanostructure film on 316L stainless steel by sol-gel dip coating. *Appl. Surf. Sci.* **2009**, *255*, 8328–8333. [[CrossRef](#)]
51. Bockmeyer, M.; Löbmann, P. Crack formation in TiO₂ films prepared by sol-gel processing: Quantification and characterization. *Thin Solid Films* **2007**, *515*, 5212–5219. [[CrossRef](#)]
52. Romankiw, L. A path: From electroplating through lithographic masks in electronics to LIGA in MEMS. *Electrochim. Acta* **1997**, *42*, 2985–3005. [[CrossRef](#)]
53. Sklar, G.P.; Paramguru, K.; Misra, M.; Lacombe, J.C. Pulsed electrodeposition into AAO templates for CVD growth of carbon nanotube arrays. *Nanotechnology* **2005**, *16*, 1265–1271. [[CrossRef](#)]
54. Zemtsova, E.; Arbenin, A.; Valiev, R.; Smirnov, V. Modern techniques of surface geometry modification for the implants based on titanium and its alloys used for improvement of the biomedical characteristics. In *Titanium in Medical and Dental Applications*; Elsevier: San Diego, CA, USA, 2018; pp. 115–145. [[CrossRef](#)]
55. Yang, J.; Chen, J.; Zhou, Y.; Wu, K. A nano-copper electrochemical sensor for sensitive detection of chemical oxygen demand. *Sens. Actuators B Chem.* **2011**, *153*, 78–82. [[CrossRef](#)]
56. Giovanelli, D.; Lawrence, N.S.; Jiang, L.; Jones, T.G.; Compton, R.G. Electrochemical determination of sulphide at nickel electrodes in alkaline media: A new electrochemical sensor. *Sens. Actuators B Chem.* **2003**, *88*, 320–328. [[CrossRef](#)]